Persistent electrical doping of $Bi_2Sr_2CaCu_2O_{8+x}$ mesa structures

Holger Motzkau, Thorsten Jacobs, Sven-Olof Katterwe, Andreas Rydh, and Vladimir M. Krasnov*
Department of Physics, Stockholm University, AlbaNova University Center, SE-106 91 Stockholm, Sweden
(Received 8 February 2012; published 18 April 2012; publisher error corrected 19 April 2012)

Application of a significantly large bias voltage to small $Bi_2Sr_2CaCu_2O_{8+x}$ mesa structures leads to persistent doping of the mesas. Here, we employ this effect for analysis of the doping dependence of the electronic spectra of Bi-2212 single crystals by means of intrinsic tunneling spectroscopy. We are able to controllably and reversibly change the doping state of *the same* single crystal from underdoped to overdoped state, without changing its chemical composition. It is observed that such physical doping is affecting superconductivity in Bi-2212 similar to chemical doping by oxygen impurities: with overdoping, the critical temperature and the superconducting gap decrease; with underdoping, the *c*-axis critical current rapidly decreases due to progressively more incoherent interlayer tunneling and the pseudogap rapidly increases, indicative for the presence of the critical doping point. We distinguish two main mechanisms of persistent electric doping: (i) even-in-voltage contribution, attributed to a charge transfer effect, and (ii) odd-in-voltage contribution, attributed to reordering of oxygen vacancies.

DOI: 10.1103/PhysRevB.85.144519 PACS number(s): 74.72.Gh, 74.62.Dh, 74.55.+v, 74.72.Kf

I. INTRODUCTION

High-temperature superconductivity (HTSC) in cuprates occurs as a result of doping of a parent antiferromagnetic Mott insulator and properties of cuprates change significantly with doping. Superconductivity in overdoped cuprates is fairly well described by the conventional BCS-type second-order phase transition.[1–3] But, properties of underdoped cuprates are abnormal due to the persistence of the normal-state pseudogap, strong superconducting fluctuations, or possibly preformed pairing,[4] and magnetism[5] at $T > T_c$. There are indications that the transition from the normal to the abnormal behavior occurs abruptly at a critical doping point.[1,6–9] This may be a consequence of the quantum phase transition: a phase transition, which occurs at $T = 0$, in frustrated systems as a result of a competition of coexisting order parameters. The coexistence of superconductivity at $T < T_c$ with the pseudogap,[10–12] charge, and spin density order[8,9,13] was indeed reported by several techniques. Clearly, detailed doping-dependent studies are needed both for understanding the puzzling nature of HTSC in cuprates and for the development of novel HTSC materials.

Usually, the mobile carrier concentration is controlled by chemical doping via chemical substitution or, in the case of cuprates, also by variation of the oxygen content via appropriate annealing and subsequent quenching to room temperature. This allows an accurate control of the chemical composition, but less so of the local arrangement of impurities and disorder, which is equally important for cuprates.[14] For example, it is well established that properties of the $YBa_2Cu_3O_{6+x}$ compound strongly depend not only on the average oxygen concentration, but also crucially on the order/disorder of oxygen atoms in Cu-O-Cu chains.[15,16] Therefore, analysis of the doping phase diagram of cuprates requires accurate control of both the concentration and the microscopic structure of impurities.

The carrier concentration can be also varied via two physical doping processes, well established for semiconductors: photodoping[17–19] and through the electric-field effect.[20–25] In the case of cuprates, physical doping may be persistent at low temperatures in a sense that it is relaxing very slowly after removing the light[17,18] or field.[21,23–25] Recently, a persistent electric doping via strong current injection was discovered.[24,25] It is resembling a resistive switching phenomenon in memristor devices[26,27] and is related to previous similar observations in point contact experiments on $Bi_2Sr_2CaCu_2O_{8+x}$ (Bi-2212).[23] Such an electric doping is reversible, reproducible, and easily controllable. It opens a possibility to analyze the doping dependence of HTSC on one sample without changing its chemical composition.[19] Despite that, there were very few direct spectroscopic studies of cuprates employing physical doping techniques.

Intrinsic tunneling spectroscopy (ITS) provides a unique opportunity to probe bulk electronic properties of HTSC.[2] This technique utilizes weak interlayer (*c*-axis) coupling in quasi-two-dimensional HTSC compounds, in which mobile charge carriers are confined in CuO_2 planes separated by some blocking layer (e.g., SrO-2BiO-SrO in case of Bi-2212). This leads to a formation of atomic-scale intrinsic tunnel junctions, and to an appearance of the intrinsic Josephson effect at $T < T_c$.[10,28–31]

In this work, we employ the persistent electric doping for analysis of the doping dependence of electronic spectra of Bi-2212 single crystals by means of intrinsic tunneling spectroscopy.[2,3,6,10,32] Controllable and reversible persistent physical doping is achieved by applying a *c*-axis voltage of a few volts to small Bi-2212 mesa structures. Thus, we are able to change the doping state of Bi-2212 single crystals without changing its chemical composition. A wide doping range from a moderately underdoped to strongly overdoped state could be reached. It is observed that the physical doping is affecting the intrinsic tunneling characteristics of Bi-2212 similar to chemical doping.[6] With overdoping, the critical temperature and the superconducting gap decrease. With underdoping, the pseudogap rapidly increases, indicative for the presence of the quantum critical doping point in the phase diagram, and the *c*-axis critical current density rapidly decreases, indicating a progressively more incoherent interlayer tunneling. We distinguish two main mechanisms of persistent electric doping: (i) an even-in-voltage contribution, attributed to a charge transfer effect, and (ii) an odd-in-voltage contribution, attributed to reordering of oxygen impurities.

The paper is organized as follows. In Sec. II, we make a brief overview of physical doping mechanisms of cuprates. Section III provides experimental details. In Sec. IV, we present the main experimental results, and in Sec. V we discuss possible mechanisms of persistent electric doping, followed by conclusions.

II. PHYSICAL DOPING OF CUPRATES

A. Photodoping

Photodoping allows a wide-range variation of doping in the same sample.[17–19] The ordinary nonequilibrium photodoping is quickly relaxing because of a very short lifetime (∼ps) of photoinduced charge carriers.[19] However, in underdoped $YBa_2Cu_3O_{6+x}$ and some other cuprates, a different type of persistent photodoping takes place.[17,18] It involves significant energies ∼1eV, which makes it metastable at low temperatures. Several mechanisms are contributing to the persistent photodoping,[33] such as charge transfer, which changes the redox state of the impurity atom,[17] and ordering of oxygen impurities in the lattice.[18] Photodoping always leads to an increase of the doping level with respect to the initial state.

B. Electric-field effects

Electric fields may both increase or decrease the number of mobile charge carriers, depending on the direction of the applied field.[20] The ordinary electric-field effect is not persistent and exists only during the time an electric field is applied. Since the electric field penetrates only to the Thomas-Fermi charge screening length, $\lambda_{TF} \lesssim 1$ nm, just a thin surface layer can be modified.[34]

A persistent electrostatic-field effect due to net electric polarization or trapped charges can be realized at the interface between a superconductor and a ferroelectric[35] or polar insulator.[36] This is also a surface phenomenon, but in the case of layered cuprates, which represent stacks of metallic CuO planes sandwiched between polar-insulating layers,[37] electrostatic charging of insulating layers may in principle lead to the *bulk* persistent electrostatic-field effect.

Another type of a persistent and bulk electric-field effect has been observed at large current densities.[21] Similar to photodoping, it was attributed to a charge transfer[38] and reordering of oxygen impurities.[22] Significant oxygen mobility in intense electric fields also leads to a resistive switching phenomenon.[23]

C. Resistive switching in complex oxides

The resistive switching phenomenon occurs in many complex oxides and is the basis for the development of resistive memory devices. Several mechanisms may be involved in the resistive switching phenomenon,[26,27] including a change of the redox state of some of the elements, oxygen migration, and filament formation. Resistive switching has been observed on depleted surfaces of Bi-2212 cuprates[23] and attributed to oxygen migration. Recently, it was demonstrated that the resistive switchinglike phenomenon can be used for controllable and reversible doping of small Bi-2212 microstructures over a wide doping range.[24,25]

III. EXPERIMENT

Mesas were fabricated on top of freshly cleaved Bi-2212 single crystals by means of optical lithography, Ar ion milling, and focused ion beam trimming. Four batches of crystals were used: pure near optimally doped (OP) Bi-2212, pure strongly underdoped (UD) Bi-2212, lead-substituted $Bi_{1.75}Pb_{0.25}Sr_2CaCu_2O_{8+\delta}$ [Bi(Pb)-2212], and yttrium-doped $Bi_2Sr_2Ca_{1-x}Y_xCu_2O_{8+\delta}$ [Bi(Y)-2212]. Mesas of different sizes from 5×5 to 1×0.5 μm^2 and with a different number of junctions $N = 8-56$ were studied. Details of the sample fabrication can be found in Ref. 39. All studied mesas exhibited a persistent doping effect upon application of a sufficiently large bias voltage.

The samples were placed in a flowing gas cryostat and measured in a three-probe configuration with a common top gold contact. The ground contacts for current and voltage were provided through other mesas on the same crystal. A Keithley K6221 current source and a FPGA-based arbitrary waveform generator and lock-in amplifier were used to bias and measure the samples. Biasing was done at pseudoconstant voltage, with an optional small superimposed ac voltage to simultaneously measure the high-bias differential resistance in addition to the dc resistance. Positive bias is defined as current going into the mesa through the common top contact, as sketched in Fig. 1(a).

IV. RESULTS

From chemical (oxygen) doping studies, it is known that doping/undoping of Bi-2212 is accompanied by a proportional decrease/increase of the c-axis resistivity.[6] Therefore, we can control the doping state by tracing the mesa resistance.

A. Dynamics of electric doping

The basic features of the dynamics of the persistent electric doping are shown in Fig. 1. Figure 1(a) shows the time evolution of the Bi(Pb)-2212 mesa resistance at a bias of ≈1.9 V at $T = 135$ K. It is seen that the mesa resistance is decreasing with time, indicating a gradual doping of the mesa. The doping rate decreases with time, following a stretched exponential decay $R = R_0 + R_d \exp[-(t/\tau)^\beta]$, shown by the dashed line in in Fig. 1(a), which is also typical for persistent photodoping.[17,18] The doping can be equally well performed at any temperature from 4 to 300 K, but the rate is increasing with T. In most cases, we perform doping at low T in order to be able to immediately probe the superconducting characteristics. Upon reduction of the bias below the threshold voltage, the state of the mesa remains stable even at room temperature on the time scale of several days.

The resistive change is reversed upon voltage reversal, as illustrated in Figs. 1(b) and 1(c) for the same Bi(Pb)-2212 mesa. The resistance decreases for positive bias (electric field into the crystal) and increases for negative bias (electric field toward the top contact), which indicates that we can controllably and reversibly dope and undope the mesa. The doping rate and direction depend both on the sign and the absolute value of bias voltage.

Figure 1(c) summarizes the bias dependence of the doping rate for the Bi(Pb)-2212 mesa. Below the threshold voltages, $|V_{dc}| \lesssim 1.7$ V, the mesa resistance is stable. Upon increasing

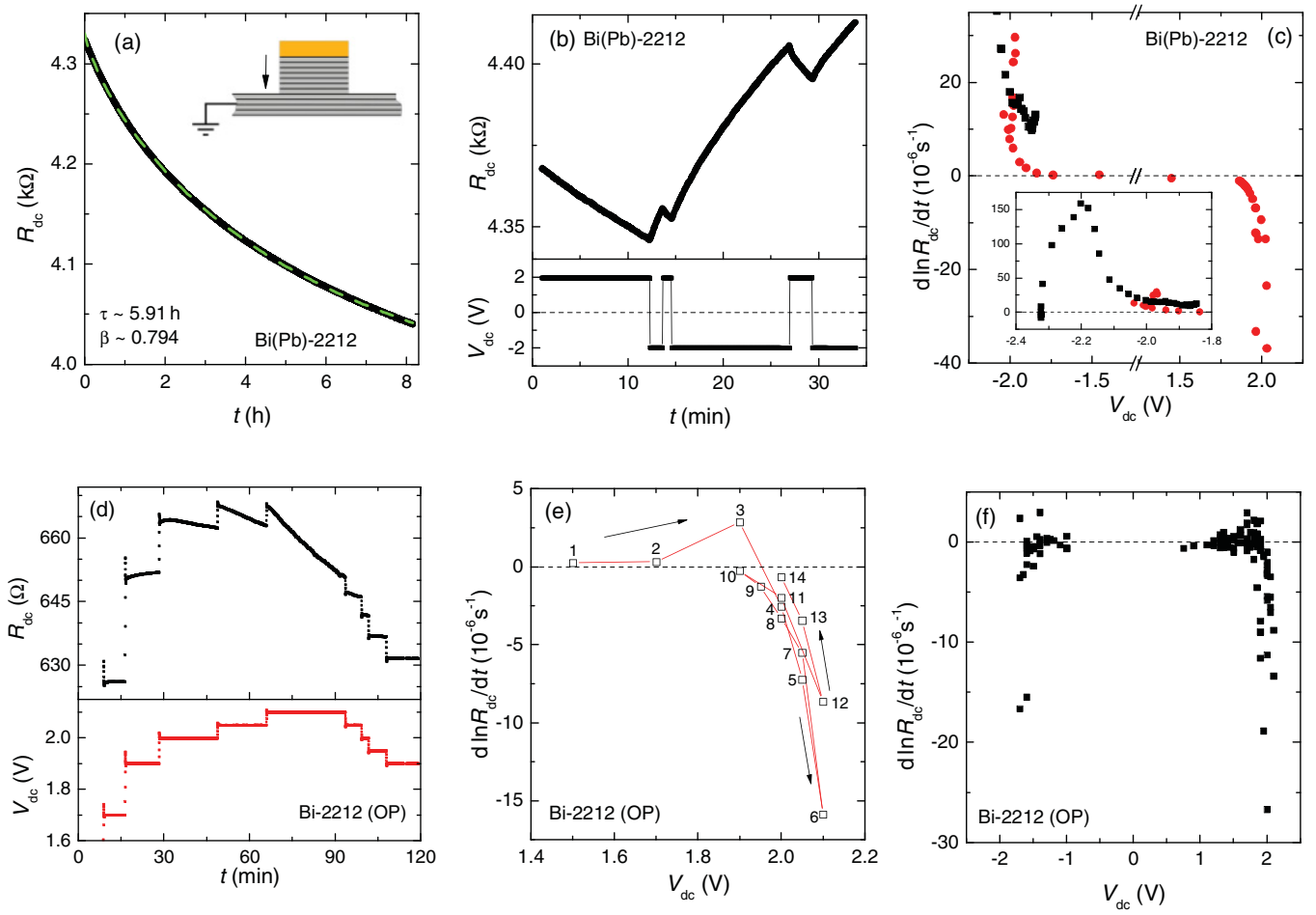

FIG. 1. (Color online) Dynamics of electric doping (a)–(c) for a Bi(Pb)-2212 mesa at $T = 135$ K and (d)–(f) for an optimally doped Bi-2212 mesa at $T = 2$ K. Panel (a) shows time evolution of the dc resistance at a bias of ≈ 1.9 V. The dashed line represents a stretched exponential decay. The inset schematically shows a sketch of a mesa structure and the direction of electric field at positive bias. (b) Demonstration of odd-in-voltage doping: the mesa resistance increases (decreases) at positive (negative) bias. Panel (c) shows the predominantly odd-voltage dependence of the logarithmic rate of the dc resistance change $d \ln R_{dc}/dt$. Different symbols represent different runs. The inset in (c) demonstrates the sign change of the doping direction at higher bias. Panel (d) demonstrates a gradual change from a negative to positive doping rate with increasing bias voltage and time. It also demonstrates a history dependence of the doping rate, i.e., a different sign of resistance change at the same bias voltage, depending on the former doping treatment. The history dependence upon several sweeps of the bias voltage is shown in (e). Panel (f) demonstrates the predominantly even-in-voltage doping for OP Bi-2212. However, an asymmetry indicates the presence of a subdominant odd-in-voltage doping. Note that despite a significant difference between the two mesas, the threshold doping voltage is similar $\sim \pm 1.7$ V (c).

the bias voltage, the resistance of the mesa starts to gradually change at a rate that increases drastically up to $|V| \sim 2.2$ V as shown in the inset of Fig. 1(c). A further voltage increase reduces the rate and then reverses the resistance alteration rate (see the inset at $V = -2.32$ V). The sign change of the alteration rate at high bias is in agreement with the observations by Koval *et al.*[24] The behavior in this regime is, however, history dependent, as may be seen from Fig. 1(c), and the final state depends on how long a time the mesas were biased at every bias voltage. The doping process for the Bi(Pb)-2212 mesa [Fig. 1(c)] is predominantly odd in bias voltage, i.e., the direction of doping is changed when the sign of the bias voltage is changed.

Figures 1(d) and 1(e) show a detailed view of the time and voltage dependence of doping for a near optimally doped pure Bi-2212 mesa. The top panel of Fig. 1(d) shows the time evolution of the resistance of an OP Bi-2212 mesa for different bias voltages, shown in the bottom panel. It is seen that the resistance is constant at $V = 1.7$ V, and starts to increase slowly at 1.9 V. However, at 2 V the resistance initially increases, but then starts to decrease after a few minutes. This clearly shows that there are two counteracting processes: a positive rate mechanism that saturates quickly and a mechanism with negative rates that is dominating at longer times and at higher voltages. The second process also saturates with time, which is clear from Fig. 1(a) and history-dependent rates of Fig. 1(e). At larger voltage, the resistance steadily decreases at a rate which is strongly bias dependent, as shown in Fig. 1(f).

Figures 1(e) and 1(f) show the bias dependence of doping and a history dependence upon sequential voltage sweeps [Fig. 1(e)]. It is seen that for the OP Bi-2212 mesa, the electric doping is predominantly even in voltage, i.e., the direction of doping does not depend on the sign of the bias voltage.

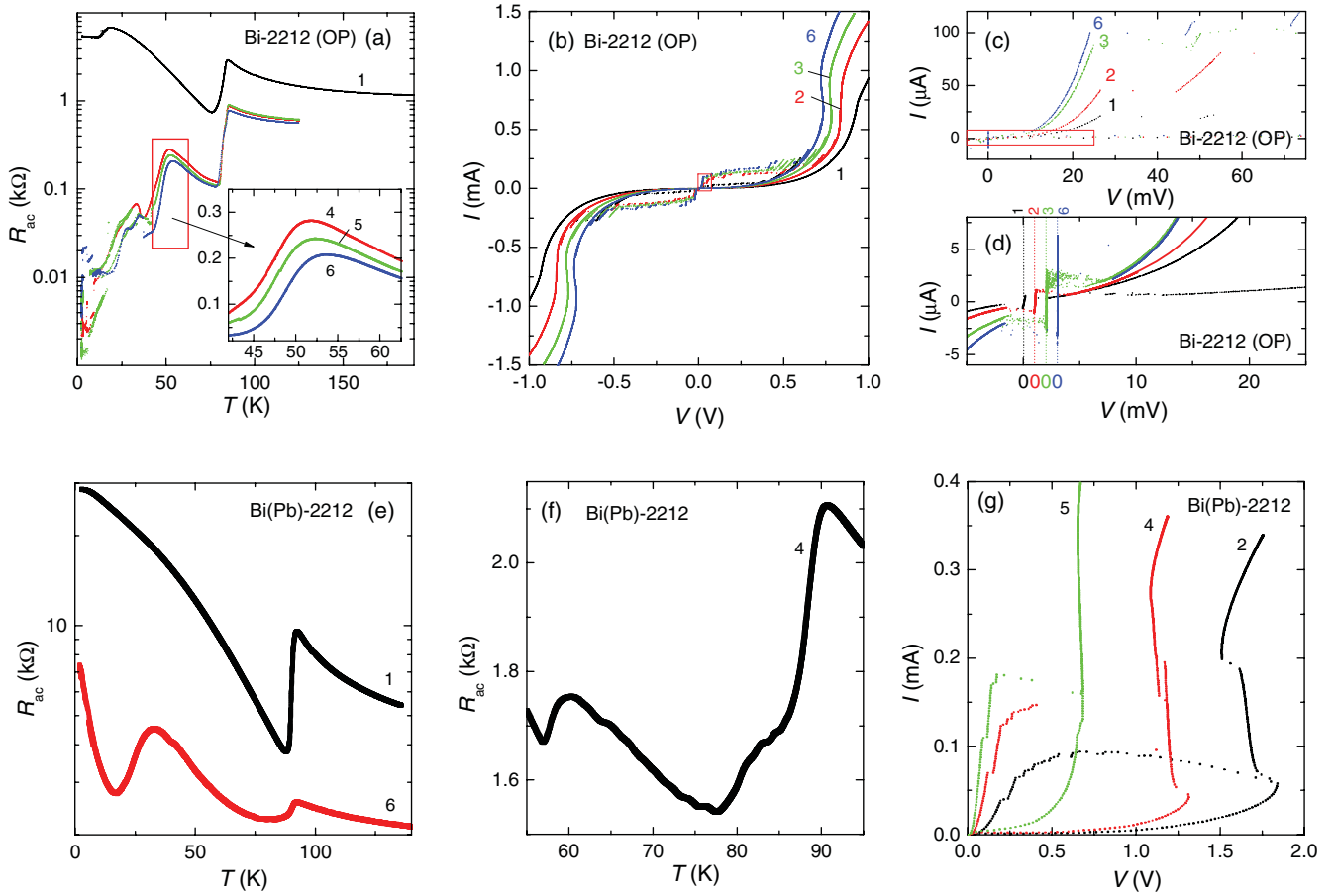

FIG. 2. (Color online) Intrinsic tunneling characteristics of the same OP Bi-2212 [(a)–(d)] and Bi(Pb)-2212 [(e)–(g)] mesas as in Fig. 1 at different doping states. (a) T dependence of the ac resistance $R_{ac}(T)$ in the initial high-resistive state 1 and subsequent low-resistance doping states 4–6. The inset illustrates the significant enhancement of T_c of the depleted surface junction. Panels (b)–(d) represent different parts of I-V characteristics in the doping states 1, 2, 3, and 6 at $T = 2$ K. A variation of the tunnel resistance, sum-gap kink, and the critical current is clearly seen. Panels (e) and (f) show $R_{ac}(T)$ for Bi(Pb)-2212 in the initial high-resistive state 1 and subsequent low-resistance doping states 4 and 6. This mesa with a large number of junctions $N = 56$ exhibits a significant spread in the T_c of individual junctions, seen as small resistance drops in (f). Panel (g) shows I-Vs of the Bi(Pb)-2212 mesa in the doping states 2, 4, and 5. A progressive increase of the critical current and decrease of the sum-gap kink voltage is seen.

However, certain asymmetry of the doping rate versus bias voltage characteristics in Figs. 2(c) and 2(f) indicates the presence of subdominant even- and odd-in-voltage contributions for Bi(Pb)-2212 and OP Bi-2212 mesas, respectively.

B. Doping dependence of ITS characteristics

Using the described method, the superconducting properties of the mesas have been altered to different intermediate doping states denoted by a successive number. The electric doping changes all mesa characteristics: the c-axis resistivity, the critical temperature T_c, the c-axis critical current density J_c, the superconducting energy gap Δ, the c-axis pseudogap, and the c-axis resistivity in a manner very similar to chemical (oxygen) doping.[6]

Figure 2 shows temperature dependencies of low-bias ac resistances for the initial, high-resistance state (HRS), and doped, lower-resistance states (LRS), for Fig. 2(a) an OP Bi-2212 and Figs. 2(e) and 2(f) a Bi(Pb)-2212 mesa. The I-V characteristics of those mesas at different doping states are presented in Figs. 2(b)–2(d) and 2(g), respectively.

From Fig. 2(a), it is seen that the initial state was characterized by the strong thermal-activation-type increase of resistance with decreasing T, typical for underdoped Bi-2212.[30] The general shape of the resistive transition was described in Ref. 2. At $T_c \sim 82$ K, the resistance dropped to the top-contact resistance, which originates from the first deteriorated junction between the top CuO plane, shortly exposed to atmosphere after cleavage, and the second, undeteriorated CuO plane.[2] Initially, this junction had a very low T_c' and a very small critical current I_c, as can be seen from the corresponding I-V in Fig. 2(d). After electric doping, the resistance in the normal state dropped almost three times and became less semiconducting. The main T_c of the mesa changed only slightly, indicating that the doping was changing around the optimal doping level with the flat T_c versus doping dependence. However, the properties of the top junction changed drastically: the T_c' increased to ~50 K, and the critical current increased tenfold as shown in Fig. 2(d), even though it still remains ~20 times smaller than for the rest of the junctions in the mesa, as can be seen from Fig. 2(c). This indicates that the surface CuO plane was initially strongly underdoped and,

therefore, responded much stronger to variation of doping, due to the steep T_c versus doping dependence at the underdoped side of the doping phase diagram of cuprates.[6] A similar trend was also observed in photodoping.[17,18]

Another possible reason for the stronger response of the underdoped top junction is the larger c-axis resistivity of underdoped intrinsic Josephson junctions.[6] Because of that, the electric field is not uniformly distributed along the mesa but is larger in the high-resistive top junction. This together with the strong voltage dependence of the electric doping leads to a faster doping of the top junction, and the doping may even go in the opposite direction with respect to the rest of the mesa.

The effect of nonuniform doping along the height of the mesa becomes more pronounced in higher mesas with a larger number of intrinsic Josephson junctions. This is seen from $R(T)$ for the Bi(Pb)-2212 mesa from Fig. 2(e), which contained a fairly large number of junctions $N \approx 56$. It is seen that after doping, some junctions retained the initial $T_c \sim 90$ K, but some were very strongly overdoped to $T_c \sim 30$ K. Figure 2(f) shows $R(T)$ at the intermediate doping state 4. Small drops represent critical temperatures of individual junctions in the mesa. Apparently, there is a gradual distribution of T_c along the height of the mesa.

Doping of Bi-2212 leads to a rapid increase of the c-axis critical current density.[6] This is clearly seen from I-V curves for the Bi-2212 (OP) mesa shown in Figs. 2(b)–2(d). The increase of I_c of the surface junction is shown in Fig. 2(d). One-by-one switching of the rest of the junctions into the resistive state at $I > I_c$ leads to the appearance of multiple-quasiparticle (QP) branch structures in the I-V curves. The corresponding critical current at the first QP branch is shown in Fig. 2(c). It also strongly increases with doping. The same effect doubles I_c in the Bi(Pb)-2212 mesa, in Fig. 2(g).

From Fig. 2(b), it is seen that the I-V curves exhibit a kink at large bias, followed by an Ohmic tunnel resistance. The kink represents the sum-gap singularity in superconducting tunnel junctions at $V = 2\Delta/e$ per junction.[2,3] This is the basis of the ITS technique, which allows analysis of the superconducting energy gap Δ in the bulk of the Bi-2212 single crystal.

Accurate analysis of the electronic spectra with the ITS technique requires mesas with a small area and a small number of identical junctions. This is needed for avoiding possible artifacts, associated with self-heating, in-plane nonequipotentiality, and spread in junction parameters.[2,40] This is particularly important for the analysis of the genuine shape of tunneling characteristics, which remains a controversial issue.[41] Even though the I-V characteristics in Figs. 2(b) and 2(g) are distorted by self-heating, as evident from a back-bending at large bias, the general trend for a variation of the sum-gap kink with doping is clearly seen: The superconducting gap decreases and the sum-gap kink becomes sharper with (over)doping. This qualitative conclusion is not affected by self-heating because the dissipation power at the kink decreases with decreasing resistance and becomes smaller with subsequent doping. Thus, with overdoping, the superconducting sum-gap singularity becomes sharper and moves to lower voltages despite the progressive reduction of self-heating. This clearly reveals the doping variation of the genuine c-axis tunneling characteristics.[41] A similar tendency was observed by other techniques, including the angular-resolved photoemission spectroscopy,[42] scanning tunneling spectroscopy,[43] and tunneling spectroscopy on point contacts,[44] as well as in previous ITS studies involving chemical (oxygen) doping.[2,6,32]

Figure 3 shows the electric doping of an initially strongly underdoped Bi-2212 mesa. A fivefold increase in critical current in the I-V characteristics [Fig. 3(a)], and an increase of T_c of about 15 K [Fig. 3(c)] can be seen. The tunneling conductance $dI/dV(V)$ curves are shown in Fig. 3(b). It is seen that the sum-gap peak shifts to slightly lower voltages and becomes sharper with doping. The hump voltage, attributed to the c-axis pseudogap,[2] rapidly decreases with increasing conductance, pointing toward an abrupt opening of the pseudogap at the critical doping point, consistent with chemical doping studies.[6,7,12]

Note that in all studied cases, the electric doping has led to a significant increase of the critical current, while the superconducting gap was decreasing. The anticorrelation between I_cR_n and Δ in underdoped Bi-2212 has been reported before[6] and was attributed to progressively more incoherent c-axis transport in combination with the d-wave symmetry of the superconducting order parameter.

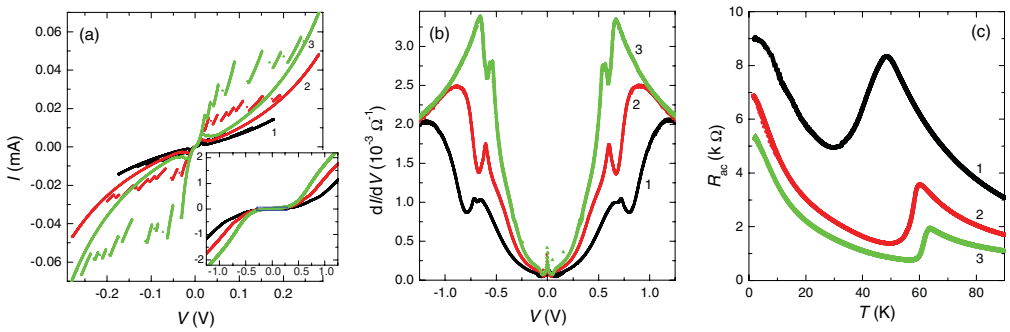

FIG. 3. (Color online) Doping of a strongly underdoped Bi-2212 mesa. (a) I-V characteristics in the initial state 1 (black) and two successive doping states 2 (red) and 3 (green). The increase of the critical current by a factor 5 is seen. (b) The corresponding dI-dV characteristics. The superconducting sum-gap peak moves to slightly lower voltages and becomes sharper with doping. The c-axis pseudogap hump voltage rapidly decreases with doping. (c) Zero-bias ac resistivity $R_{ac}(T)$. The T_c has increased by about 15 K in the state 3.

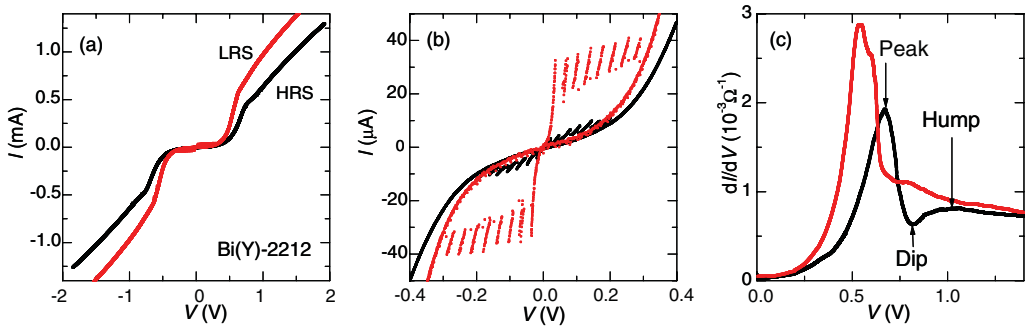

FIG. 4. (Color online) Intrinsic tunneling characteristics of a small Bi(Y)-2212 mesas at low T before (slightly underdoped, HRS) and after (optimally doped, LRS) doping by a short voltage pulse. Panels (a) and (b) show I-V curves at a large scale and at the quasiparticle branches, respectively. A reduction of the high-bias tunnel resistance and a simultaneous increase of the critical current in the doped state is seen. Panel (c) shows dI/dV ITS characteristics. A change in the shape of the curves is seen: the peak becomes sharper and the dip hump less pronounced in the optimally doped state, compared to the initial underdoped state.

C. Short-pulse doping

So far, we were discussing a gradual electric doping of Bi-2212 mesas at the time scale of an hour, as shown in Fig. 1. Such a long time doping allows a very strong variation of the doping state, but often leads to inhomogeneous doping within the mesa height, as shown in Fig. 2. Koval *et al.*[25] demonstrated that a short-pulse doping strategy leads to highly reversible and reproducible doping, similar to resistive switching in point contacts.[23] This is probably related to the lack of significant electromigration during the short pulse, which may eventually lead to an irreversible destruction of the crystal structure.[21]

Figure 4 represents the ITS characteristics at $T \sim 30$ K for a small $\sim 2 \times 2$ μm^2 Bi(Y)-2212 mesa with a small amount of junctions and small self-heating.[40] In the initial high-resistive state, the mesa is slightly underdoped with $T_c \sim 91$ K. The mesa was switched to a low-resistive state by a short voltage pulse $V \gtrsim 2$ V of about a milliseconds width. The periodicity of QP branches in Fig. 4(b) demonstrates that after switching into the LRS, the mesa remains highly uniform. From comparison of I-V curves in Figs. 4(a) and 4(b), it is seen that the decrease of resistance by $\sim 1/3$ is accompanied by an almost fourfold increase of I_c. The T_c increased to $\sim$93 K being an indication that the mesa became near optimally doped.

Figure 4(c) represents the tunneling conductance dI/dV in the high-resistive (underdoped) and the low-resistive (optimally doped) states. The following main changes in ITS spectra are seen: the superconducting sum-gap peak voltage decreased in the doped low-resistive state and the shapes of spectra are changed. The relative sum-gap peak height $dI/dV(V_p)R_n$ is increased by about 50% in the low-resistive state. The high-resistive state exhibits a peak-dip-hump structure, which is less obvious in the low-resistive state. All this is similar to the slow-doping case (Figs. 2 and 3), and consistent with the change of doping from the slightly underdoped to near optimally doped state,[6] in accordance with other spectroscopic studies involving chemical (oxygen) doping.[42–44]

As already discussed above, the increase of sharpness of the sum-gap kink in the I-V curve and the peak in the dI/dV curve in the low-resistive state, reported in Figs. 2 and 4, and the change of the shape of the peak-dip-hump feature in Fig. 4(c) can not be attributed to self-heating because the actual power dissipation at the peak is decreasing in the low-resistive state. For example, the corresponding powers at the peaks in Fig. 4(c) are $P = 0.21$ and 0.17 mW, respectively. This observation supports the conclusion of Ref. 41 that the appearance and the shape of the peak-dip-hump structure in the ITS characteristics of small mesas is determined primarily by the doping level.

A detailed analysis of short-pulsed resistive switching has been performed on strongly underdoped Bi-2212 mesas. For negative pulses with 50 μs length and compliance voltages up to -2.5 V, there was no resistive switching. At -3.0 V, a reduction of the quasiparticle resistance to 99.3% is observed (LRS). Nine subsequent pulses reduce the resistance further to 98.4%. A single positive pulse switches the resistance back to the initial HRS, while more positive pulses do not result in additional changes. A single negative pulse with a higher compliance voltage of -3.5 V instead reduces the resistance of the LRS to about 93.4% of the HRS, and the corresponding positive pulses switch it back. Pulses with lower compliance voltage lead to a partial switching, but additional pulses with the same compliance do not lead to a significant change. Figure 5(a) shows I-V curves of another UD Bi-2212 mesa at $T = 2$ K in the HRS and the LRS obtained with a 3.5-V pulse of 50 μs width. The general difference between I-V's after the pulsed doping in Figs. 4(a) and 5(a) is the same as for the slow doping in Figs. 2(a) and 3(a).

Figure 5(b) demonstrates a reproducible resistive switching between HRS and LRS at elevated $T = 100$ K for another UD Bi-2212 mesa. The switching was performed using a similar positive and negative pulse sequence with ± 3.5 V, a pulse width of 100 μs, and an interval between pulses of 3 s, shown in the bottom panel of Fig. 5(b). Figures 5(b) and 5(c) show the corresponding time sequence of the measured zero-bias resistance of the mesa. It is seen that negative voltage pulses lead to switching into the LRS, while a subsequent positive pulse switches the mesa back into the HRS. The corresponding resistance change rates are of the order of $d \ln R/dt \approx \mp 1000$ s^{-1}, which are somewhat higher than for the slow doping shown in Fig. 1(d), but not inconsistent with that data, taking into account that the compliance voltage is also significantly higher. It is seen that the HRS is stable and shows no visible relaxation at $T = 100$ K, while the LRS is initially relaxing with the characteristic time $\tau_{LRS} = (0.77 \pm 0.30)$ s and then saturates before reaching the HRS, as shown in

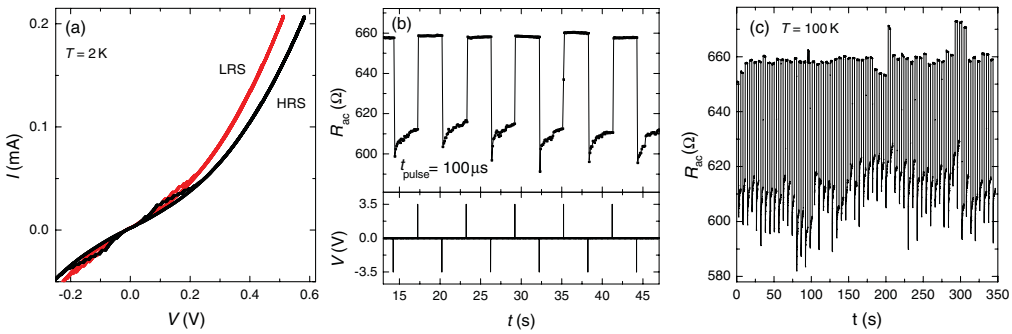

FIG. 5. (Color online) Short-pulse resistive switching in a strongly underdoped Bi-2212 mesa. (a) I-V characteristics in the initial high-resistive state (HRS) and the doped low-resistive state (LRS) at $T = 2$ K. Panels (b) and (c) demonstrate the resistive switching sequence R_{ac} versus time at $T = 100$ K. The switching was made by a train of short positive and negative pulses, shown in the bottom of panel (b). It is seen that the HRS is stable, but the LRS is initially relaxing and then saturates at a resistance below the HRS. Several hundred reproducible resistive switching events can be achieved without visible degradation (c).

Fig. 5(b). At $T = 280$ K, the behavior is similar with a time constant of $\tau_{LRS} = (0.75 \pm 0.34)$ s.

V. DISCUSSION: MECHANISMS OF PERSISTENT ELECTRIC DOPING

In Sec. II, we briefly reviewed known mechanisms of persistent physical doping of cuprates. It is likely that some of them are playing a role in persistent electric doping, studied here. Indeed, the phenomenon is clearly related to the persistent electric-field effect,[21] observed in $YBa_2Cu_3O_{6+x}$, which in turn is clearly related to persistent photodoping observed for various cuprates.[17,18]

To identify possible mechanisms, we first summarize characteristic features of the persistent electric doping:

(1) Observed different voltage dependencies (odd and even) indicate that several distinct mechanisms are involved.

(2) The doping rate shows a thresholdlike behavior as a function of bias voltage (see Fig. 1). The threshold voltage depends on T in a thermal-activation manner, i.e. decreases with increasing T. Remarkably, the threshold voltage is weakly dependent on the number of junctions in the mesa, consistent with previous reports,[24,25] and is comparable to that for a single point contact.[23] This suggests that the phenomenon is connected to some characteristic energy $\sim$1 eV, rather than directly to the electric field. Indeed, for a given voltage, the latter should scale inversely proportional to the number of junctions in the mesa, i.e., would not be universal for different mesas (that is why we hesitate to refer to the phenomenon as a persistent electric-*field* effect, and rather call it persistent electric doping).

(3) However, the role of the electric field should not be underestimated. Indeed, the displacement field is given by $D = V\varepsilon_r/Nt$, where ε_r is the dielectric constant and t is the thickness of the insulating barrier between CuO bilayers. The ratio $t/\varepsilon_r \simeq 0.1$ nm was estimated from an analysis of Fiske (geometrical resonance) step voltages.[31] Therefore, the displacement field in intrinsic junctions is

$$D \simeq \frac{V}{N} \times 10^8 \text{ cm}^{-1}. \quad (1)$$

For $V \simeq 2$ V and $N \simeq 10$, which corresponds to the case of Fig. 4, one would get a very large value $D \simeq 2 \times 10^7$ V/cm, which is certainly capable of seriously polarizing and displacing ions in complex oxides.[21,23,26]

(4) The phenomenon is not associated with a net change of the oxygen content, which may only decrease within the cryostat. To the contrary, mesas can be repeatedly and reversibly doped and undoped, as shown in Figs. 1(b) and 5(b).

A. Charge transfer and electrostatic charge trapping

If an injected electron has a high enough energy, it may join one of the ions, leading to a change of the redox state and the effective doping. It was suggested that such a "charge transfer" mechanism is involved both in photodoping of cuprates[17] and in the resistive switching phenomenon in other complex oxides.[26]

Alternatively, the electron may be trapped (localized) in dielectric parts, leading to electrostatic charging of the sample. The Bi-2212 compound has a layered structure with metallic CuO planes sandwiched between polar insulator BiO layers.[37] In this case, the electrostatic charging will take place in BiO layers, which may affect the doping state of the neighboring CuO planes via the electrostatic-field effect. The electrostatic charging of means by current injection takes place uniformly within the whole structure. Therefore, unlike the conventional electric-field effect[20] and the electrostatic-field effect at the interface between a superconductor and a ferroelectric material,[35,36] the current injection may lead to a persistent *bulk* electrostatic field-effect doping of Bi-2212. Koval *et al.*[24] emphasized the similarity of the phenomenon with the floating-gate effect utilized in Flash memory devices.

Both types of charging effects have common similarities: (i) The charge transfer requires a certain energy ($\sim$eV for $YBa_2Cu_3O_{6+x}$), rather than electric field. (ii) The sign of the current and the direction of the electric field does not matter. Therefore, such doping should be even with respect to the voltage sign, consistent with the observations in Ref. 24. Therefore, we attribute even-in-voltage persistent electric doping to charge transfer and/or charge trapping mechanisms.

B. Oxygen reorientation and reordering

It is well established that the doping state of cuprates depends not only on the amount of off-stoichiometric oxygen, but also on the relative orientation of the oxygen bonds.[15] Therefore, the doping state can be changed by oxygen reordering. Since the required energy is large ∼eV, compared to thermal energies, oxygen reordering is a slow process and does not take place spontaneously at low enough T. Oxygen reordering is considered as one of the main mechanisms of the persistent photodoping[18] and electric-field[21] doping.

In the case of persistent electric-field doping, the oxygen reordering is steered by the polarization. Therefore, the direction of doping should depend on the direction of the electric field, i.e., should be odd with respect to the bias voltage. We clearly see such a contribution in our experiment [see Fig. 1(b)]. Note that the odd-in-voltage contribution was reported in the point-contact case,[23] but not reported in previous related works made on zigzag-type Bi-2212 microstructures.[24,25] The geometry of the latter samples is symmetric with respect to the electric-field direction (changing the sign of the electric field is equivalent to flipping their sample upside down). This is not the case in point contacts and mesa structures, studied here, for which the fields down (into the crystal) and up (into the top electrode) are not equivalent. Therefore, the difference may partly be due to the difference in sample geometry, or to the observed sample dependence of the relative strength of odd- and even-in-voltage doping contributions, as shown in Figs. 1(d) and 1(e). Thus, we attribute the odd-in-voltage persistent electric doping mechanism to field-induced oxygen reorientation/reordering.

C. Irreversible processes: Electromigration, filament, and arc formation

An increase of the bias voltage above ∼2.5−3.0 V leads to a gradual increase of the current and irreversible change of the mesa properties. A similar phenomenon was observed in $YBa_2Cu_3O_{6+x}$ thin films and attributed to electromigration and field-induced diffusion of oxygen, which is even in bias voltage. The increase of conductance is probably due to a dielectric breakthrough in the insulating BiO layers, which leads to a pin-hole and filament formation. Thus, we attribute the slow and irreversible drift of the mesa characteristics at large bias voltages to electromigration in the mesas. This destructive process is, however, distinctly different from the reversible and reproducible electric doping effect, reported above.

After deterioration by electromigration, the mesa characteristics become similar to resistive switching characteristics for point contacts on top of oxygen-depleted, Bi-2212 surfaces.[23] At even higher bias, the resistance becomes very high (infinite). But, an inspection in a microscope shows that the mesa itself remains intact. There is no physical evaporation of material or a crater at the place of the mesa, as in the case of a violent electric discharge. Instead, there are clear indications of an arc formation at one of the sharp corners of the mesa, which probably leads to delamination of the structure and mechanical disattachment of the mesa from the base crystal.

D. Mechanisms of energy accumulation

The most puzzling property of the reported persistent electric doping is that the required bias voltage is weakly dependent on the number of junctions in the mesa.[24,25] This is clearly seen from the presented data, for which the threshold voltage is always ∼2V for $N = 9$ in Fig. 4, $N = 11$ in Fig. 1(f), and $N \sim 56$ in Fig. 1(d), which is also similar to that for a single point contact ∼1.5 V.[23] It is, therefore, clear that electric doping requires a certain electron energy, rather than electric field. However, for stacked tunnel junctions, the energy acquired by the injected electron in every tunneling event is proportional to the voltage drop across the junction, $\delta E \simeq eV/N$, and is significantly smaller than the threshold energy. The main question is, therefore, how the electrons accumulate a sufficiently large energy, required for doping.

In Ref. 25, it was suggested that an electron can accumulate energy upon sequential tunneling through several junctions without relaxation. However, in this case, only electrons in the last junction will have enough energy. This would result in a strongly inhomogeneous doping in different junctions. Moreover, the probability of sequential tunneling without relaxation is small because of the small ratio of relaxation time ($\tau \sim$ ps) (Ref. 45) to the tunnel time $t_{\rm tun}$, $t_{\rm tun}/\tau \gg 1$. The probability of sequential tunneling through N junctions is decreasing rapidly $\propto (\tau/t_{\rm tun})^N$ with increasing N. This should lead to a dramatic increase of the doping time with increasing N. Indeed, suppose that it takes $t_N \sim 10$ min for N junctions at $I = 1$mA to dope the mesa. This will involve $N_e = It_N/e$ tunneling events in each junction (e is the electron charge). Since the probability of sequential tunneling through $2N$ junctions is decreasing quadratically, it would require N_e^2 tunneling events per junction, which will take $t_{2N} = N_e t_N = 3.75 \times 10^{19}$min. However, such a dramatic increase of the doping time with increasing mesa height is inconsistent with experiments.

For the sequential tunneling scenario to be relevant, the ratio $t_{\rm tun}/\tau$ should rapidly drop with increasing electron energy and become of the order of unity at $E \sim 1$ eV. This may be caused by resonant tunneling, which increases the tunneling rate of quasiparticles with a certain energy and/or by a drastic slowing down of the high-energy quasiparticle relaxation, which may be caused by a rapid decrease of the Eliashberg's electron-boson spectral function and a gap in the corresponding bosonic density of states at high energies.[45] Such a scenario is interesting to investigate because it may give information about the bosonic spectrum, involved in Cooper pairing, and thus provide a clue about the electron-boson coupling mechanism, responsible for high-T_c superconductivity in cuprates.[45]

We also want to propose an alternative mechanism for the energy accumulation of electrons: the formation of electric-field domains in the natural atomic superlattice formed by the mesa. Electric-field domains are well studied in semiconducting superlattices.[46] They appear in weakly coupled superlattices close to the resonant tunneling condition. The corresponding nonlinearity leads to an instability and multiple-valued current-voltage characteristics. As a result, the electric-field distribution in the superlattice becomes nonuniform and is concentrated in one or several junctions.

A possibility of a formation of electric-field domains in Bi-2212 mesas is not just a hypothesis. In fact, the multiple-branch I-V of Bi-2212 mesas due to one-by-one switching of intrinsic junctions from the superconducting to the resistive state, shown in Fig. 4(b), is due to a formation of electric-field domains in individual tunnel junctions. The formation of electric-field domains in Bi-2212 mesas at high bias would explain many of the features of the studied persistent electric doping. In this case, electrons in the domain may gain an energy close to eV without sequential tunneling through the whole mesa. Furthermore, since domains are typically dynamic and propagate through the whole superlattice,[46] this would also explain the uniformity of doping in the whole mesa, and not just in the outermost junction.

VI. CONCLUSIONS

We have studied the effect of persistent electric doping on intrinsic tunneling characteristics of small Bi-2212 mesa structures. It was shown that the application of a sufficiently large voltage to the mesas leads to a controllable and reversible physical doping of the mesas, without a modification of their chemical composition. This allows the analysis of bulk electronic spectra in Bi-2212 in a wide doping range on one and the same mesa. This physical doping has the same effect as chemical (oxygen) doping on the intrinsic tunneling characteristics of Bi-2212: the c-axis resistivity decreases, the critical current increases, and the energy gap is decreasing together with T_c with overdoping. The anticorrelation between I_cR_n and Δ indicates that the c-axis transport becomes progressively more incoherent at the underdoped side of the phase diagram. An analysis of the doping variation of the intrinsic tunneling characteristics of the same mesa provides a clue about its genuine shape: with subsequent doping, the sum-gap peak in the tunneling conductance becomes sharper and the pseudogap hump rapidly decreases with doping, suggesting the presence of a critical doping point, in agreement with previous chemical doping studies.[6]

By analyzing the bias and time dependence, we could identify different mechanisms involved in the persistent electric doping: (i) the even-in-voltage process via charge transfer and/or charge trapping, and (ii) the odd-in-voltage process via oxygen reordering. Those are distinct from the irreversible electromigration and oxygen electrodiffusion, observed at higher bias.

We confirm the previous report[25] that the threshold voltage for the electric doping is weakly dependent of the number of junctions in the mesas and is similar to that for a single surface point contact.[23] This indicates that it is the energy of injected electrons, rather than electric field, that determines the phenomenon. We suggest that the required energy accumulation by tunnel electrons may be due to a formation of electric-field domains in the natural atomic superlattice formed in the Bi-2212 single crystal.

ACKNOWLEDGMENT

We are grateful to the Swedish Research Council and the SU-Core Facility in Nanotechnology for financial and technical support.

*Vladimir.Krasnov@fysik.su.se

[1] J. L. Tallon and J. W. Loram, Phys. C (Amsterdam) **349**, 53 (2001).
[2] V. M. Krasnov, Phys. Rev. B **79**, 214510 (2009).
[3] V. M. Krasnov, H. Motzkau, T. Golod, A. Rydh, S. O. Katterwe, and A. B. Kulakov, Phys. Rev. B **84**, 054516 (2011).
[4] T. Kondo, Y. Hamaya, A. D. Palczewski, T. Takeuchi, J. S. Wen, Z. J. Xu, G. Gu, J. Schmalian, and A. Kaminski, Nat. Phys. **7**, 21 (2011).
[5] R.-H. He, M. Hashimoto, H. Karapetyan, J. D. Koralek, J. P. Hinton, J. P. Testaud, V. Nathan, Y. Yoshida, H. Yao, K. Tanaka, W. Meevasana, R. G. Moore, D. H. Lu, S.-K. Mo, M. Ishikado, H. Eisaki, Z. Hussain, T. P. Devereaux, S. A. Kivelson, J. Orenstein, A. Kapitulnik, and Z. X. Shen, Science **331**, 1579 (2011).
[6] V. M. Krasnov, Phys. Rev. B **65**, 140504(R) (2002).
[7] F. F. Balakirev, J. B. Betts, A. Migliori, I. Tsukada, Y. Ando, and G. S. Boebinger, Phys. Rev. Lett. **102**, 017004 (2009).
[8] T. Helm, M. V. Kartsovnik, M. Bartkowiak, N. Bittner, M. Lambacher, A. Erb, J. Wosnitza, and R. Gross, Phys. Rev. Lett. **103**, 157002 (2009).
[9] D. LeBoeuf, N. Doiron-Leyraud, B. Vignolle, M. Sutherland, B. J. Ramshaw, J. Levallois, R. Daou, F. Laliberte, O. Cyr-Choiniere, J. Chang, Y. J. Jo, L. Balicas, R. Liang, D. A. Bonn, W. N. Hardy, C. Proust, and L. Taillefer, Phys. Rev. B **83**, 054506 (2011).
[10] V. M. Krasnov, A. Yurgens, D. Winkler, P. Delsing, and T. Claeson, Phys. Rev. Lett. **84**, 5860 (2000).
[11] W. S. Lee, I. M. Vishik, K. Tanaka, D. H. Lu, T. Sasagawa, N. Nagaosa, T. P. Devereaux, Z. Hussain, and Z. X. Shen, Nature (London) **450**, 81 (2007).
[12] L. Yu, D. Munzar, A. V. Boris, P. Yordanov, J. Chaloupka, Th. Wolf, C. T. Lin, B. Keimer, and Ch. Bernhard, Phys. Rev. Lett. **100**, 177004 (2008).
[13] R. Daou, J. Chang, D. LeBoeuf, O. Cyr-Choiniere, F. Laliberte, N. Doiron-Leyraud, B. J. Ramshaw, R. Liang, D. A. Bonn, W. N. Hardy, and L. Taillefer, Nature (London) **463**, 519 (2010).
[14] K. Fujita, T. Noda, K. M. Kojima, H. Eisaki, and S. Uchida, Phys. Rev. Lett. **95**, 097006 (2005).
[15] N. Chandrasekhar, O. T. Valls, and A. M. Goldman, Phys. Rev. B **49**, 6220 (1994).
[16] M. Käll, M. Osada, M. Kakihana, L. Börjesson, T. Frello, J. Madsen, N. H. Andersen, R. Liang, P. Dosanjh, and W. N. Hardy, Phys. Rev. B **57**, 14072(R) (1998).
[17] V. I. Kudinov, I. L. Chaplygin, A. I. Kirilyuk, N. M. Kreines, R. Laiho, E. Lähderanta, and C. Ayache, Phys. Rev. B **47**, 9017 (1993).
[18] A. Gilabert, A. Hoffmann, M. G. Medici, and I. K. Schuller, J. Supercond. Novel Magn. **13**, 1 (2000).
[19] D. Fausti, R. I. Tobey, N. Dean, S. Kaiser, A. Dienst, M. C. Hoffmann, S. Pyon, T. Takayama, H. Takagi, and A. Cavalleri, Science **331**, 189 (2011).

[20]C. H. Ahn, A. Bhattacharya, M. Di Ventra, J. N. Eckstein, C. D. Frisbie, M. E. Gershenson, A. M. Goldman, I. H. Inoue, J. Mannhart, A. J. Millis, A. F. Morpurgo, D. Natelson, and J.-M. Triscone, Rev. Mod. Phys. **78**, 1185 (2006).

[21]B. H. Moeckly, D. K. Lathrop, and R. A. Buhrman, Phys. Rev. B **47**, 400 (1993); S. H. Huerth, H. D. Hallen, and B. Moeckly, *ibid.* **67**, 180506(R) (2003).

[22]P. Konsin and B. Sorkin, Phys. Rev. B **58**, 5795 (1998).

[23]N. A. Tulina, G. A. Emelchenco, and A. B. Kulakov, Phys. Lett. A **204**, 74 (1995); N. A. Tulina, A. M. Ionov, and A. N. Chaika, Phys. C (Amsterdam) **366**, 23 (2001); A. Plecenik, M. Grajcar, P. Seidel, S. Takacs, A. Matthes, M. Zuzcak, and S. Benacka, *ibid.* **301**, 234 (1998).

[24]Y. Koval, X. Jin, C. Bergmann, Y. Simsek, L. Özyüzer, P. Müller, H. Wang, G. Behr, and B. Büchner, Appl. Phys. Lett. **96**, 082507 (2010).

[25]Y. Koval, F. Chowdhury, X. Jin, Y. Simsek, F. Lichtenberg, R. Pentcheva, and P. Müller, Phys. Status Solidi A **208**, 284 (2011).

[26]R. Waser and M. Aono, Nat. Mater. **6**, 833 (2007); R. Waser, R. Dittmann, M. Salinga, and M. Wuttig, Solid–State Electron. **54**, 830 (2010).

[27]J. J. Yang, M. D. Pickett, X. Li, D. A. A. Ohlberg, D. R. Stewart, and R. S. Williams, Nat. Nanotechnol. **3**, 429 (2008).

[28]R. Kleiner and P. Müller, Phys. Rev. B **49**, 1327 (1994).

[29]K. Anagawa, Y. Yamada, T. Watanabe, and M. Suzuki, Phys. Rev. B **67**, 214513 (2003).

[30]S. O. Katterwe and V. M. Krasnov, Phys. Rev. B **80**, 020502(R) (2009).

[31]S. O. Katterwe, A. Rydh, H. Motzkau, A. B. Kulakov, and V. M. Krasnov, Phys. Rev. B **82**, 024517 (2010).

[32]S. O. Katterwe, A. Rydh, and V. M. Krasnov, Phys. Rev. Lett. **101**, 087003 (2008).

[33]N. Kristoffel and P. Rubin, Phys. C (Amsterdam) **418**, 49 (2005).

[34]B. Y. Shapiro, Solid State Commun. **56**, 149 (1985).

[35]R. Aidam, D. Fuchs, and R. Schneider, Phys. C (Amsterdam) **328**, 21 (1999).

[36]A. Walkenhorst, C. Doughty, X. X. Xi, Q. Li, C. J. Lobb, S. N. Mao, and T. Venkatesan, Phys. Rev. Lett. **69**, 2709 (1992); X. X. Xi, J. Supercond. **7**, 137 (1994).

[37]S. O. Katterwe, H. Motzkau, A. Rydh, and V. M. Krasnov, Phys. Rev. B **83**, 100510(R) (2011).

[38]M. Salluzzo, G. Ghiringhelli, J. C. Cezar, N. B. Brookes, G. M. DeLuca, F. Fracassi, and R. Vaglio, Phys. Rev. Lett. **100**, 056810 (2008).

[39]V. M. Krasnov, T. Bauch, and P. Delsing, Phys. Rev. B **72**, 012512 (2005).

[40]V. M. Krasnov, M. Sandberg, and I. Zogaj, Phys. Rev. Lett. **94**, 077003 (2005).

[41]V. M. Krasnov, Phys. Rev. B **84**, 136501 (2011).

[42]H. Ding, J. R. Engelbrecht, Z. Wang, J. C. Campuzano, S.-C. Wang, H.-B. Yang, R. Rogan, T. Takahashi, K. Kadowaki, and D. G. Hinks, Phys. Rev. Lett. **87**, 227001 (2001).

[43]K. M. Lang, V. Madhavan, J. E. Hoffman, E. W. Hudson, H. Eisaki, S. Uchida, and J. C. Davis, Nature (London) **415**, 412 (2002).

[44]L. Ozyuzer, J. F. Zasadzinski, K. E. Gray, C. Kendziora, and N. Miyakawa, Europhys. Lett. **58**, 589 (2002).

[45]V. M. Krasnov, Phys. Rev. Lett. **97**, 257003 (2006); **103**, 227002 (2009).

[46]L. L. Bonilla and H. T. Grahn, Rep. Prog. Phys. **68**, 577 (2005).